Astronomy & Astrophysics manuscript no. H2O-final
December 26, 2011

© ESO 2011

arXiv:1112.4850v2 [astro-ph.SR] 23 Dec 2011

Letter to the Editor

Detection of warm water vapour in Taurus protoplanetary discs by Herschel

P. Riviere-Marichalar[1], F. Ménard[2], W. F. Thi[2], I. Kamp[3], B. Montesinos[1], G. Meeus[4], P. Woitke[5,6,7], C. Howard[8], G. Sandell[8], L. Podio[3], W. R. F. Dent[9], I. Mendigutía[1], C. Pinte[2], G.J. White[10,11], D. Barrado[1,12]

(Affiliations can be found after the references)

ABSTRACT

Line spectra of 68 Taurus T Tauri stars were obtained with the *Herschel-PACS (Photodetector Array Camera & Spectrometer)* instrument as part of the *GASPS (Gas Evolution in Protoplanetary Systems)* survey of protoplanetary discs. A careful examination of the linescans centred on the [OI] 63.18 μm fine-structure line unveiled a line at 63.32 μm in some of these spectra. We identify this line with the $8_{18} \rightarrow 7_{07}$ transition of ortho-water. It is detected confidently (i.e., $> 3\sigma$) in eight sources, i.e., ~ 24% of the sub-sample with gas-rich discs. Several statistical tests were used to search for correlations with other disc and stellar parameters such as line fluxes of [O I] 6300Å and 63.18 μm; X-ray luminosity and continuum levels at 63 μm and 850 μm. Correlations are found between the water line fluxes and the [O I] 63.18 μm line luminosity, the dust continuum, and possibly with the stellar X-ray luminosity. This is the first time that this line of warm water vapour has been detected in protoplanetary discs. We discuss its origins, in particular whether it comes from the inner disc and/or disc surface or from shocks in outflows and jets. Our analysis favours a disc origin, with the observed water vapour line produced within 2-3AU from the central stars, where the gas temperature is of the order of 500-600K.

Key words. Stars: formation, astrobiology, astrochemistry, line: identification, molecular data, protoplanetary discs.

1. Introduction

Discs are natural by-products of star formation and the birthplaces of planets. One of the key questions intimately linked with planet formation and the concept of planet habitability is how much vapour and icy water is present in discs and how it is radially distributed. However, it is only recently that observations of water vapour in discs have become possible.

Carr & Najita (2008), using the *Spitzer* InfraRed Spectrograph (IRS), reported a rich molecular emission-line spectrum dominated by rotational transitions of hot water from the disc of AA Tau. They concluded that the molecular emission seen in the mid-IR has a most likely origin within the 2-3 AU inner regions of the disc. Salyk et al. (2008) detected water emission in the 10-20 μm region with Spitzer-IRS, as well as water and hydroxyl emission around 3 μm with *NIRSPEC* on *Keck II*, for both DR Tau and AS 205 A. The emission comes from the disc atmospheres of the objects and the excitation temperatures were found to be (~ 1000 K), which is typical of terrestrial planet formation regions. Pontoppidan et al. (2010b) performed a survey for more protoplanetary discs in Ophiuchus, Lupus, and Chamaeleon, again with *Spitzer-IRS*, and concluded that the presence of mid-IR molecular emission lines, including those of water, is a common phenomenon in discs around Sun-like stars. Also, Pontoppidan et al. (2010a) presented a sample of ground-based observations of pure rotational lines of water vapour in the protoplanetary discs of AS 205 A and RNO 90 that was analysed to measure line widths of 30–60 km s^{-1}, which is consistent with an origin in a disc in Keplerian rotation at a radius of ~ 1 AU, and gas temperatures in the range 500–600 K.

The *Herschel Space Observatory* (Pilbratt et al. 2010) has opened the far-IR window with unprecedented sensitivity, allowing astronomers to survey the atomic and molecular gas content of disc regions that are cooler than those probed by *Spitzer* and ground-based instruments. Predictions of the water lines detectable by Herschel can be found in Cernicharo et al. (2009) and Woitke et al. (2009b). Hogerheijde et al. (2011) presented the first detection of cold water in the disc of the ~10 Myr old TW Hya, using *Herschel-HIFI*. The *Herschel* Open Time Key Program *GASPS (Gas Evolution in Protoplanetary Systems)* (Mathews et al. 2010) is conducting a survey to measure gas lines and continuum in ~250 discs around low- and intermediate-mass stars with ages in the range 1-30Myr with PACS, the *Photodetector Array Camera & Spectrometer* (Poglitsch et al. 2010).

In this letter, we report the first detection of the o-H_2O line at 63.32 μm in a subsample of protoplanetary discs around T Tauri stars in the 1-3 Myr old Taurus star forming region.

2. Observations and data reduction

This study is based on a sample of 68 classical and weak-line T Tauri stars from the Taurus star forming region with spectral measurements from *Herschel*-PACS centred at the wavelength of the [O I] $^3P_1 \rightarrow ^3P_2$ 63.184 μm line. The Taurus star-forming region is one of the main targets for the study of protoplanetary systems, because it is among the nearest star-forming regions (d = 140 pc) with a well-known population of more than 300 young stars and brown dwarfs according to Kenyon et al. (2008), Luhman et al. (2010), and Rebull et al. (2010).

The observations described in this letter are part of the *Herschel* Open Time Key Programme *GASPS* [P.I. W. Dent], (Mathews et al. 2010, see), a flux-limited survey devoted to the study of the gas and dust in circumstellar systems around young stars. The survey focuses on the detection of the [O I] emission at the 63.18 μm feature. For this study, we analyzed 68 stars with spectral types ranging from late F-early G to mid M. The PACS spectral observations were made in chop/nod pointed line mode. The observing times ranged from 1215 to 6628 seconds, depending on the number of nod cycles. The data were reduced using HIPE 7.0.1751. A modified version of the PACS pipeline

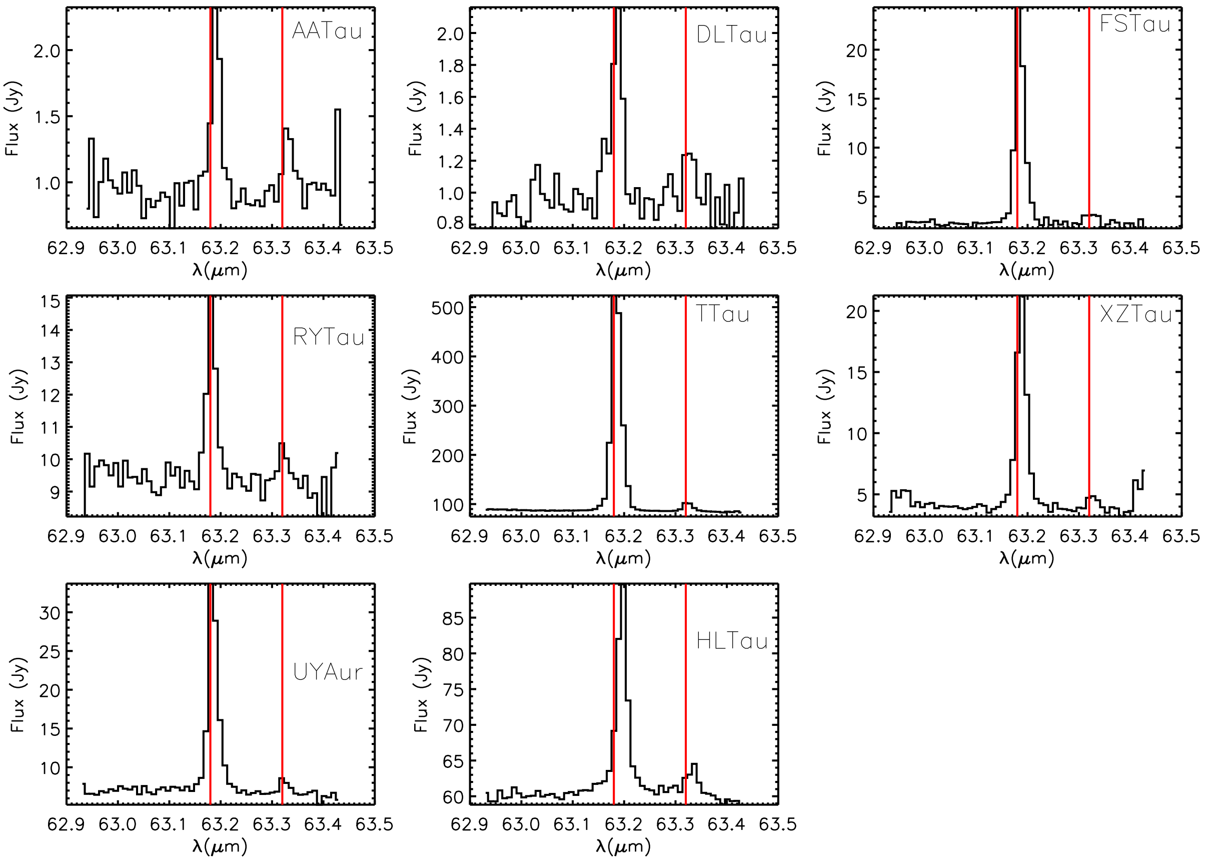

Fig. 1. Spectra for the objects with a 63.32μm feature detection ($> 3\sigma$). The red lines indicate the rest wavelength of the [O I] and o-H_2O emission.

was used, which included: saturated and bad pixel removal, chop subtraction, relative spectral response-function correction, and flat fielding. Many observations suffer from systematic pointing errors, in some cases as large as 8″, and are always shifted to the East. This is due to a plate scale error in the star tracker, which is normally negligible except in areas where the tracked stars are asymmetrically distributed within the field, as in Taurus. The mis-pointing translates into systematic small shifts in the line centre position. When the star was well centred within a single spaxel, we extracted the flux from that spaxel and applied the proper aperture correction. When the flux was spread over more than one spaxel, we co-added the spaxels.

Table 1. Line positions and fluxes from PACS spectra.

Name	Sp. type	$\lambda_{H_2O} - \lambda_{[OI]}$	[O I] flux	$o - H_2O$ flux
–	–	μm	10^{-17} W/ m^2	10^{-17} W/m^2
AA Tau	K7	0.140	2.2 ± 0.13	0.80 ± 0.13
DL Tau	K7	0.141	2.4 ± 0.15	0.65 ± 0.14
FS Tau	M0	0.139	37 ± 0.26	2.00 ± 0.33
RY Tau	K1	0.139	10 ± 0.42	1.95 ± 0.38
T Tau	K0	0.138	830 ± 0.75	27.8 ± 0.7
XZ Tau	M2	0.139	32.2 ± 0.48	2.11 ± 0.48
HL Tau	K7	0.142	54.3 ± 0.71	8.14 ± 0.80
UY Aur	M0	0.139	33.6 ± 0.37	1.90 ± 0.32

Notes. All spectral types from the compilation of Luhman et al. (2010).

3. Results and discussion.

Among the sample of 68 Taurus targets studied in this letter, 33 have discs that are rich in gas. These 33 all show the [O I] $^3P_1 \rightarrow ^3P_2$ line in emission at 63.18 μm (signal-to-noise ratio > 3, with values ranging from 3 to 375). In 8 of these 33 targets (~ 24%), an additional fainter emission-line at 63.32 μm is detected (Fig.1). We computed 63.32 μm line fluxes by fitting a gaussian plus continuum curve to the spectrum using DIPSO [1]. To improve the line fitting, the noisier edges of the spectral range were removed (i.e., $\lambda < 63.0$ and $\lambda > 63.4$). The results are listed in Table 1, where we report the peak position of the feature with respect to the observed wavelength of the [O I] 63.18 μm line. According to these fits, the peak of the feature is at $\lambda_0 = 63.32$ μm. The FWHM is 0.020 μm, i. e., the instrumental FWHM for an unresolved line. We identify the feature as the ortho-H_2O $8_{18} \rightarrow 7_{07}$ transition at 63.324 μm ($E_{\mathrm{Upper\ Level}}$=1070.7 K, Einstein A=1.751 s^{-1}) since no other abundant species emit strongly at or close to the observed wavelength of the feature. This water feature was observed by Herczeg et al. (2011) in the outflow of NGC 1333 IRAS 4B.
The o-H_2O emission is only present in spectra with [O I] detections. The targets FS Tau, HL Tau, and T Tau display extended emission in the [O I] 63.18 μm line, but only T Tau show hints of extended emission in the 63.32μm o-H_2O line. T Tau is an exceptional object. It is a triple star system that drives at least two jets. It was the most line rich PMS star observed by ISO (Lorenzetti 2005) and resembles more a hot core than a PMS star, since the continuum emission is quite extended (~ 3.5 ″at

---

[1] http://star-www.rl.ac.uk/docs/sun50.htx/sun50.html

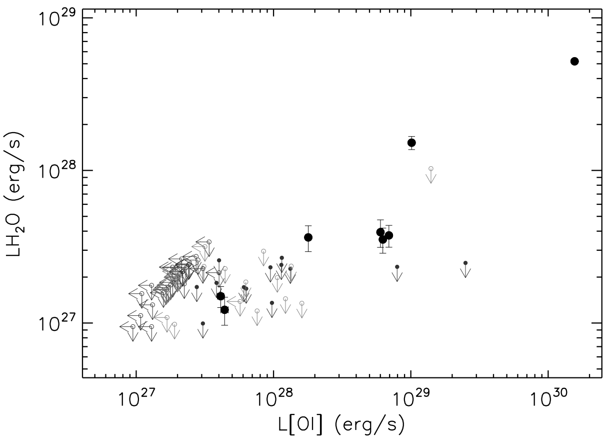

Fig. 2. Plot of the 63.32 μm o-H_2O line luminosity versus [OI] 63.18 μm. Filled dots are detections, arrows are upper limits. Solid, dark grey arrows represent objects with non-detections spanning the same spectral range as the objects with detections. Light grey, empty arrows represent non-detections with other spectral types.

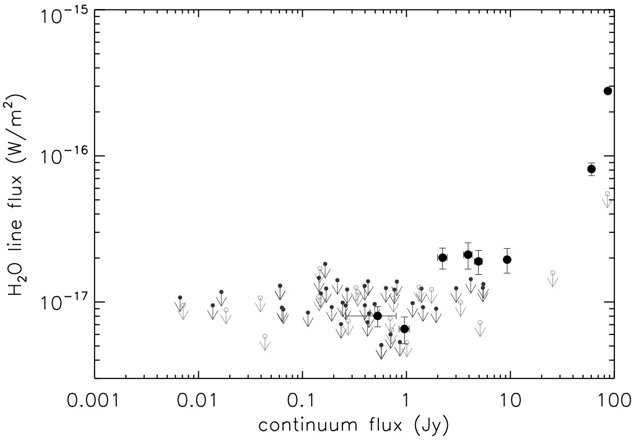

Fig. 3. Plot of the 63.32 μm ortho-H_2O line flux versus 63μm continuum flux. Symbols as in Fig. 2.

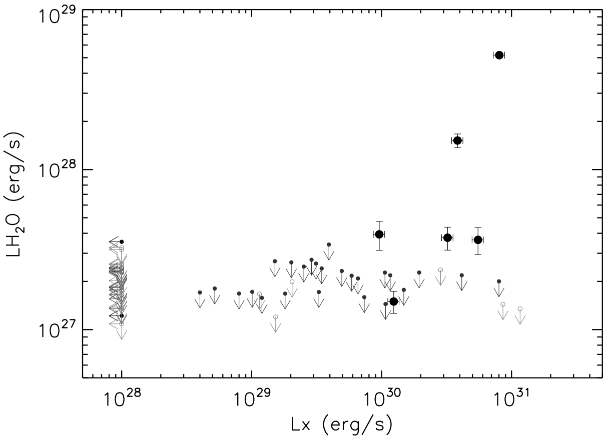

Fig. 4. H_2O luminosity versus X-ray luminosity. Symbols as in Fig. 2.

Table 2. Probabilities for correlations between o-H_2O line intensity and stellar/disc parameters.

Observable	Points n	Spearman's prob.	Kendall's prob.
$L_{[OI]}$	68	0.0009 (0.4090)	0.0000 (0.196)
63 μm flux	64	0.0147 (0.2635)	0.0002 (0.4567)
850 μm flux $^{(2)}$	57	0.0145 (0.2596)	0.0131 (0.8496)
L_{star} $^{(3)}$	65	0.1789 (0.1130)	0.1980 (0.5535)
L_X $^{(3)}$	65	0.0225 (0.9912)	0.0087 (0.6012)
$\alpha(2\mu m - 8\mu m)$ $^{(4)}$	62	0.026 (0.1547)	0.0023 (0.3850)
$L_{[OI]6300Å}$	27	0.1291 (0.3255)	0.1008 (0.3450)

Notes. The values obtained for random populations are shown in brackets. Accurate only if N > 30. (2): 850 μm continuum fluxes from Andrews & Williams (2005). (3): Values from Güdel et al. (2007). (4): SED slope from Luhman et al. (2010).

70 μm). It is impossible to tell how much of the line emission comes from the discs, from the outflows, or even from the surrounding envelope.

To help us understand the origin of the o-H_2O emission, we compared the line intensity with several star and disc (jet) parameters. We computed survival analysis ranked statistics using the ASURV code (Feigelson & Nelson 1985; Isobe et al. 1986). The result of this analysis is summarised in Table 2. We also created random populations to test the validity of the results.

The survival analysis shows a correlation between the o-H_2O line fluxes and the [O I] line fluxes at a significance level of 0.99 (see Fig. 2). This relationship suggests that both lines have a similar origin. The H_2O emission is correlated with the continuum emission at 63 μm, but at a significance level of 0.95 in the Spearman statistics (Fig. 3). The 850 μm continuum flux can be used as a proxy for the amount of dust present in the disc. A survival analysis shows a possible correlation with the 850 μm continuum flux, at a significance level of 0.95 in both Spearman and Kendall statistics, although a large scatter is present. A correlation with neither the stellar luminosity nor the spectral type is found. There seems to be a weak correlation with the slope of the SED measured between 2 μm and 8 μm, used as a proxy for the presence of hot dust. The significance of this correlation is dominated by T Tau, which has the highest o-H_2O flux in the sample. There is likely no link between mass loss rate and L_{H_2O}. The [O I] luminosity at 6300 Å is proportional to the mass loss rate (Hartigan et al. 1995). Although the sample is too small to test this relationship conclusively, we note that while $L_{[OI]6300Å}$ spans four orders of magnitude, the H_2O luminosity spans only one order of magnitude. Finally, the survival analysis statistics points to a possible relationship with the X-ray luminosity L_x (Fig. 4). While the Spearman probability for the real sample is only one order of magnitude smaller than for the random sample, the Kendall probability is two orders of magnitude smaller. Inspection of Fig. 4 also shows that the o-H_2O line flux is detected only for sources with X-ray luminosities higher than 10^{30} erg s^{-1}, which is consistent with photochemical disc models that show that far-IR line fluxes increase significantly above this X-ray luminosity threshold (Aresu et al. 2011). We note that $\log L_x = 10^{30}$ erg s^{-1} is above the median (mean) X-ray luminosity in Taurus ($\log L_x = 29.8$ (29.75) erg s^{-1} respectively, Güdel et al. (2007)). Interestingly, more than half of the sources with $L_x > 10^{30}$ erg s^{-1} do not display the o-H_2O line. This behaviour may stem from either (1) the different shape of the X-ray spectrum (hardness ratio), (2) the duty cycle of the flares responsible for the high levels of X-ray fluxes, and/or (3) that X-rays are not the only driver of H_2O chemistry and excitation, let alone any inner disc geometry and radiative transfer considerations. We caution that the correlation with X-rays is significantly weaker when TTau is removed from the analysis.

All the stars detected in o-H_2O are outflow/jet sources, although three of them AA Tau, DL Tau, and RY Tau do not show any excess in [OI], i.e. all the emission is consistent with coming from the disc (Howard et al., in prep). Two of these (AA Tau and DL Tau) are classified as outflow sources based on blue-shifted forbidden optical emission lines, although the emission is only slightly blue-shifted for AA Tau. However, in the sample there are also some prominent jet sources ($L_{[OI]6300Å} > 10^{-2}$ $L_{\odot}$) that show no hint of emission from this o-H_2O line, such as DG Tau, where other H_2O lines have been detected. However, these H_2O lines are believed to originate in the outflow. Furthermore, the [OI] at 63.18 μm line is sometimes extended (Podio et al. in prep, Herczeg et al. 2011), while we find the o-H_2O to be unresolved, suggesting a more compact origin for the o-H_2O line.

We therefore assume that the o-H_2O emission at 63.32 μm originates from the disc and ask whether it comes from the same gas reservoir as the hot H_2O lines observed by Spitzer. Carr & Najita (2011) detected six out of eleven stars: AA Tau, BP Tau, DK Tau, GI Tau, RW Aur, and UY Aur. Our sample contains all of their detected sources. We detected the 63.32 μm H_2O emission only in AA Tau and UY Aur. Pontoppidan et al. (2010b) reported H_2O detections toward three out of eight stars in their sample: DR Tau, AA Tau, and IQ Tau. We did not detect o-H_2O in IQ Tau. Salyk et al. (2008), Pontoppidan et al. (2009) and Meijerink et al. (2009) argued that the *Spitzer* hot H_2O emission comes from the 0.1 to 1.0 AU annular region of the disc.

Assuming the same temperature, column density, and emitting areas as Carr & Najita (2011), i.e., 1AU, we computed the 63.32μm LTE line flux in AA Tau and UY Aur. The model line emission is too optically thick to derive the H_2O mass reliably. The size of the emitting region is instead estimated. In both cases, the model flux is ten times lower than measured. To recover the measured fluxes, the radius of the emitting area has to be about three times larger than the value they quote, i. e., 3.0 AU for AA Tau and 3.5 AU for UY Aur, a result that is consistent with the lower excitation temperature of the line we observed.

A radiation thermo-chemical model of a typical T Tauri disc obtained with the ProDiMo code (Woitke et al. 2009a; Kamp et al. 2010; Thi et al. 2010; Aresu et al. 2011) predicts that the emission region of the 63.32 μm o-H_2O line is of the order of 3 AU, about five times larger than the Spitzer emission-line region (see Fig. B.1). One particular o-H_2O line at 15.738 μm was selected as a representative Spitzer mid-IR H_2O emission line. This model does not intend to fit any particular object. A large non-LTE H_2O ro-vibrational model calculation was included to consistently calculate the Spitzer as well as the Herschel H_2O emission lines by applying escape probability theory (Faure et al. 2004, 2007; Faure & Josselin 2008). At $\sim$ 3 AU, the gas densities are high enough to excite the 63.32 μm o-H_2O line and the dust temperature close to the mid-plane is low enough for H_2O to freeze onto grains.

The 63.32 μm line could provide the missing link between the mid-IR Spitzer detections of hot H_2O vapour in T Tauri discs and the cold far-IR H_2O lines observed with *Herschel*. Searches for the lower excitation H_2O lines have proven to be less successful. To date, the only clear detection of cold H_2O from a disc is TW Hya using *HIFI* (Hogerheijde et al. 2011) , and Kamp et al. (in prep.), using *PACS*. Possible reasons for the lower detection rate of cold H_2O might be the much lower H_2O abundances in the outer disc caused by the freeze-out of H_2O and/or significant (vertical) settling of icy grains (Bergin et al. 2010). Observing the same molecule in transitions with very different excitation temperatures may trace it through a broader range of different radial zones in protoplanetary discs.

4. Conclusions

We have detected o-H_2O emission at 63.32 μm in 8 T Tauri stars in a sub-sample of 68 stars located in Taurus. The detection rate is ~24% in the sub-sample with gas-rich discs. The H_2O emission appears to be correlated with the continuum luminosities, the [O I] 63.18 μm line fluxes, and the X-ray luminosities. The gas temperature (500-600K) and density needed to excite the observed o-H_2O line suggest that the line is coming from the inner parts of the discs and from the upper layers of its atmosphere, where the disc is directly illuminated. The correlation with X-rays flux and the role of X-ray emission in heating the gas, in particular during flares, needs to be investigated further. The typical size of the emitting region is estimated to be $r \sim$ 3 AU, which is consistent with the typical location of the snow line in these objects. More effort is needed to detect several H_2O lines simultaneously in more objects to understand the full radial distribution of H_2O vapour in planet-forming discs.

Acknowledgements. We thank the anonymous referee for a constructive report that helped to improve the paper. This research has been funded by Spanish grants AYA 2010-21161-C02-02, CDS2006-00070 and PRICIT-S2009/ESP-1496. In France we thank ANR (contracts ANR-07-BLAN-0221 and ANR-2010-JCJC-0504-01); CNES; PNPS of CNRS/INSU. The Millennium Science Initiative (ICM) of the Chilean ministry of Economy (Nucleus P10-022-F) and an EC-FP7 grant (PERG06-GA-2009-256513) are also acknowledged.

References

Andrews, S. M. & Williams, J. P. 2005, ApJ, 631, 1134
Aresu, G., Kamp, I., Meijerink, R., et al. 2011, A&A, 526, A163+
Bergin, E. A., Hogerheijde, M. R., Brinch, C., et al. 2010, A&A, 521, L33+
Carr, J. S. & Najita, J. R. 2008, Science, 319, 1504
Carr, J. S. & Najita, J. R. 2011, ApJ, 733, 102
Cernicharo, J., Ceccarelli, C., Ménard, F., Pinte, C., & Fuente, A. 2009, ApJ, 703, L123
Faure, A., Crimier, N., Ceccarelli, C., et al. 2007, A&A, 472, 1029
Faure, A., Gorfinkiel, J. D., & Tennyson, J. 2004, MNRAS, 347, 323
Faure, A. & Josselin, E. 2008, A&A, 492, 257
Feigelson, E. D. & Nelson, P. I. 1985, ApJ, 293, 192
Güdel, M., Briggs, K. R., Arzner, K., et al. 2007, A&A, 468, 353
Hartigan, P., Edwards, S., & Ghandour, L. 1995, ApJ, 452, 736
Herbig, G. H. & Bell, K. R. 1988, Third Catalog of Emission-Line Stars of the Orion Population : 3 : 1988, ed. Herbig, G. H. & Bell, K. R.
Herczeg, G. J., Karska, A., Bruderer, S., et al. 2011, ArXiv e-prints
Hogerheijde, M. R., Bergin, E. A., Brinch, C., et al. 2011, ArXiv e-prints
Isobe, T., Feigelson, E. D., & Nelson, P. I. 1986, ApJ, 306, 490
Kamp, I., Tilling, I., Woitke, P., Thi, W.-F., & Hogerheijde, M. 2010, A&A, 510, A18
Kenyon, S. J., Gómez, M., & Whitney, B. A. 2008, Low Mass Star Formation in the Taurus-Auriga Clouds, ed. Reipurth, B., 405–+
Lorenzetti, D. 2005, Space Sci. Rev., 119, 181
Luhman, K. L., Allen, P. R., Espaillat, C., Hartmann, L., & Calvet, N. 2010, ApJS, 186, 111
Mathews, G. S., Dent, W. R. F., Williams, J. P., et al. 2010, A&A, 518, L127+
Meijerink, R., Pontoppidan, K. M., Blake, G. A., Poelman, D. R., & Dullemond, C. P. 2009, ApJ, 704, 1471
Pilbratt, G. L., Riedinger, J. R., Passvogel, T., et al. 2010, A&A, 518, L1+
Poglitsch, A., Waelkens, C., Geis, N., et al. 2010, A&A, 518, L2+
Pontoppidan, K. M., Meijerink, R., Dullemond, C. P., & Blake, G. A. 2009, ApJ, 704, 1482
Pontoppidan, K. M., Salyk, C., Blake, G. A., & Käufl, H. U. 2010a, ApJ, 722, L173
Pontoppidan, K. M., Salyk, C., Blake, G. A., et al. 2010b, ApJ, 720, 887
Rebull, L. M., Padgett, D. L., McCabe, C.-E., et al. 2010, ApJS, 186, 259
Salyk, C., Pontoppidan, K. M., Blake, G. A., et al. 2008, ApJ, 676, L49
Thi, W.-F., Woitke, P., & Kamp, I. 2010, MNRAS, 407, 232
Woitke, P., Kamp, I., & Thi, W.-F. 2009a, A&A, 501, 383
Woitke, P., Thi, W.-F., Kamp, I., & Hogerheijde, M. R. 2009b, A&A, 501, L5

Appendix A: Non detections

GASPS is a flux-limited survey. All sources have detection limits for the o-H_2O line at 63.32 μm around 10^{-17} W/m^2, with an uncertainty of a factor of two both ways. The list of non detections is given in table A.1.

Appendix B: Location of emission for H_2O lines

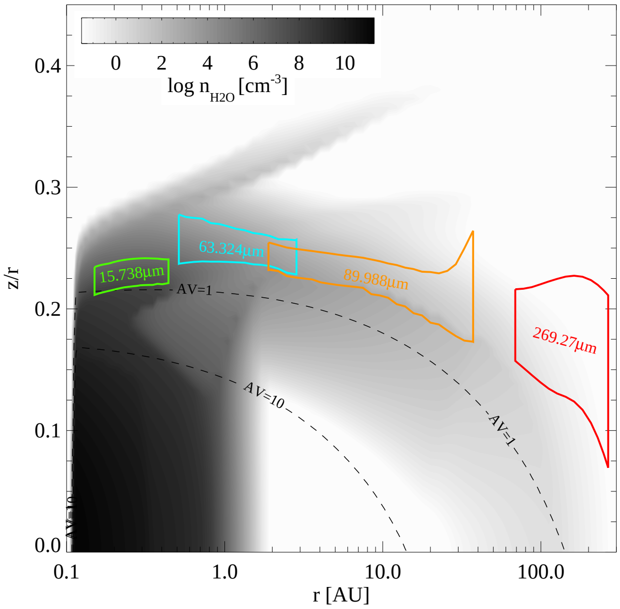

Fig. B.1. Location of the H_2O emission for a typical disc model (M_*=0.8M$_\odot$, L_*=0.7 L$_\odot$, $T_{\rm eff}$=4400K, UV excess $f_{\rm UV}$=0.01, X-ray luminosity L_X=10^{30} erg s^{-1}, $R_{\rm in}$=0.1AU, $R_{\rm out}$=300 AU, $M_{\rm disc}$=0.01 M$_\odot$, dust/gas=0.01, ϵ=-1, scale height H_0=1 AU at r_0=10 AU, flaring β = 1.1, astronomical silicate with uniform dust size distribution $a_{\rm min}$=0.05 μm, $a_{\rm max}$=1 mm, and index=3.5.). The 15.738 μm line is used as a typical H_2O line detected by *Spitzer*. We have marked the radii where the cumulative line flux reaches 15% and 85% with vertical lines, for the four selected H_2O lines. In addition, the horizontal lines mark the heights above the midplane where 15% and 85% of the line flux, from every vertical column, originate in. The encircled regions are hence responsible for 70% x 70% = 49% of the total line flux (for a pole-on disc).

---

[1] Centro de Astrobiología – Depto. Astrofísica (CSIC–INTA), POB 78, 28691 Villanueva de la Cañada, Spain
e-mail: `riviere@cab.inta-csic.es`
[2] UJF-Grenoble 1 / CNRS-INSU, Institut de Planétologie et d'Astrophysique (IPAG) UMR 5274, Grenoble, F-38041, France
[3] Kapteyn Astronomical Institute, P.O. Box 800, 9700 AV Groningen, The Netherlands
[4] Dep. de Física Teórica, Fac. de Ciencias, UAM Campus Cantoblanco, 28049 Madrid, Spain
[5] University of Vienna, Dept. of Astronomy, Türkenschanzstr. 17, A-1180 Vienna, Austria
[6] UK Astronomy Technology Centre, Royal Observatory, Edinburgh, Blackford Hill, Edinburgh EH9 3HJ, UK
[7] SUPA, School of Physics & Astronomy, University of St. Andrews, North Haugh, St. Andrews KY16 9SS, UK
[8] SOFIA-USRA, NASA Ames Research Center
[9] ALMA, Avda Apoquindo 3846, Piso 19, Edificio Alsacia, Las Condes, Santiago, Chile
[10] Department of Physics & Astronomy, The Open University, Milton Keynes MK7 6AA, UK
[11] The Rutherford Appleton Laboratory, Chilton, Didcot, OX11 OQL, UK
[12] Calar Alto Observatory, Centro Astronómico Hispano-Alemán C/Jesús Durbán Remón, 2-2, 04004 Almería, Spain

Table A.1. Source list, spectral types, and 63.32 μm o-H_2O line fluxes.

Name	SP. Type	$o - H_2O$ flux
–	–	10^{-17} W/m^2
Anon 1	M0	<1.17
BP Tau	K7	<0.94
CIDA2	M5.5	<0.89
CI Tau	K7	<0.92
CoKu Tau/4	K3	<1.37
CW Tau	K3	<1.26
CX Tau	M2.5	<0.94
CY Tau	M1.5	<1.41
DE Tau	M1	<1.23
DF Tau	M2	<1.28
DG Tau	K6?	<1.32
DG Tau B	< K6	<1.25
DH Tau	M1	<1.07
DK Tau	K6	<0.53
DL Tau	K7	<1.14
DM Tau	M1	<0.89
DN Tau	M0	<0.77
DO Tau	M0	<1.21
DP Tau	M0.5	<0.92
DQ Tau	M0	<0.98
DS Tau	K5	<0.58
FF Tau	K7	<1.11
FM Tau	M0	<1.24
FO Tau	M3.5	<0.96
FQ Tau	M3	<0.91
FT Tau	–	<1.25
FW Tau	M5.5	<1.08
FX Tau	M1	<1.82
GG Tau	M5.5	<1.24
GH Tau	M2	<0.84
GIK Tau	K7	<0.74
GM Aur	K7	<1.21
GO Tau	M0	<1.23
Haro 6-13	M0	<1.43
Haro6-37	M1	<1.84
HBC 347	K1[1]	<1.69
HBC 356	K2[1]	<0.94
HBC 358	M3.5	<1.29
HK Tau	M0.5	<0.90
HN Tau	K5	<0.64
HO Tau	M0.5	<1.46
HV Tau	M1	<0.72
IP Tau	M0	<0.83
IQ Tau	M0.5	<1.38
04158+2805	M5.25	<1.06
LkCa 1	M4	<1.06
LkCa 3	M1	<0.94
LkCa 4	K7	<0.98
LkCa 5	M2	<1.16
LkCa 7	M0	<0.88
LkCa 15	K5	<0.52
SAO 76428	F8?	<1.58
SU Aur	G2	<0.72
UX Tau	K5	<0.99
UZ Tau	M2	<0.60
V710 Tau	M0.5	<1.17
V773 Tau	K3	<0.77
V819 Tau	K7	<1.21
V927 Tau	M4.75	<0.88
VY Tau	M0	<1.30

Notes. Spectral types from the compilation by Luhman et al. (2010).
(1): from Herbig & Bell (1988)